High-temperature single-molecule kinetic analysis of thermophilic archaeal MCM helicases

Kelly M. Schermerhorn[1], Nathan Tanner[1,*], Zvi Kelman[2] and Andrew F. Gardner[1,*]

[1]New England Biolabs, Ipswich, MA 01938, USA and [2]Biomolecular Labeling Laboratory, National Institute of Standards and Technology and Institute for Bioscience and Biotechnology Research, University of Maryland, Rockville, MD 20850, USA

ABSTRACT

The minichromosome maintenance (MCM) complex is the replicative helicase responsible for unwinding DNA during archaeal and eukaryal genome replication. To mimic long helicase events in the cell, a high-temperature single-molecule assay was designed to quantitatively measure long-range DNA unwinding of individual DNA helicases from the archaeons *Methanothermobacter thermautotrophicus* (Mth) and *Thermococcus* sp. 9°N (9°N). Mth encodes a single MCM homolog while 9°N encodes three helicases. 9°N MCM3, the proposed replicative helicase, unwinds DNA at a faster rate compared to 9°N MCM2 and to Mth MCM. However, all three MCM proteins have similar processivities. The implications of these observations for DNA replication in archaea and the differences and similarities among helicases from different microorganisms are discussed. Development of the high-temperature single-molecule assay establishes a system to comprehensively study thermophilic replisomes and evolutionary links between archaeal, eukaryal, and bacterial replication systems.

INTRODUCTION

Chromosomal DNA helicases play an essential role in all domains of life by unwinding duplex DNA ahead of replication forks. The replicative helicase in eukarya and archaea is termed the minichromosome maintenance (MCM) complex (1–4). The ring-shaped hexameric MCM complex encircles the leading strand and moves along single-stranded DNA (ssDNA) in the 3'-5' direction, unwinding the duplex DNA ahead of the replication fork [reviewed in (4)]. In eukarya, MCM is a heterohexamer comprised of six related polypeptides (Mcm2-7), while in most archaeal species, MCM is a homohexamer (5,6). The structure and function of MCM from several archaeal species have been extensively studied [reviewed in (4)]. The archaeal MCM consists of a N-terminal region involved in hexamer formation and DNA binding and a C-terminal region containing the catalytic domains and a helix-turn-helix (HTH) motif. The archaeal MCM uses the energy from ATP hydrolysis to unwind duplex DNA and is a major component of the replisome. Most archaea encode a single MCM while a subset encodes both a replicative helicase and additional MCM homologs. Extra MCM homologs are typically located in mobile elements, are not linked to genes that encode other known replisome proteins and are not essential for viability (7,8).

During chromosomal DNA replication, MCM unwinds long stretches of genomic DNA. However, most helicase assays use short oligonucleotide substrates, and therefore cannot accurately capture processive unwinding events. To better analyze and mimic *in vivo* replication, we developed a single-molecule helicase assay capable of monitoring long, processive helicase unwinding events. This high-temperature single-molecule assay uses a flow cell chamber containing long (>40 kb) DNA constructs tethered to polystyrene beads under laminar flow (9–11). The rate and distance of the movement of a tethered magnetic bead against flow is directly related to the DNA unwinding rate and processivity of an active helicase, utilizing the intrinsic length contrast between of single- and double-stranded DNA under low forces. Single-molecule assays directly measure helicase activity, allowing observation of transient states and rare events that cannot be observed in bulk experiments that average many events [reviewed in (12)].

In this work, the assay is used to study the rates and processivities of thermostable MCM helicases from *Methanothermobacter thermautotrophicus* (Mth) and *Thermococcus* sp. 9°N (9°N). Mth is an anaerobic thermophilic euryarchaeon isolated from sewage sludge that encodes a single MCM homolog (5,6,13,14). 9°N is an anaerobic hyperthermophilic euryarchaeon isolated from scrapings of a deep sea volcanic smoker chimney collected at the 9°N East Pacific Rise vent site, 500 miles south of Acapulco, Mexico at a depth of 2500 m (15). Many 9°N replication proteins including DNA polymerase B, DNA polymerase D, flap en-

*To whom correspondence should be addressed. Tel: +1 978 927 5054; Fax: +1 978 921 1350; Email: gardner@neb.com
Correspondence may also be addressed to Nathan Tanner. Email: tanner@neb.com

donuclease 1 and DNA ligase have been studied and assigned roles in replication and Okazaki fragment maturation (16,17). 9°N encodes three MCM homologs designated 9°N MCM1, 9°N MCM2 and 9°N MCM3. 9°N MCM3 is proposed to function as the replicative helicase since it is 93% identical to the essential replicative MCM3 from *Thermococcus kodakarensis* (Tko), is encoded in an operon with the GINS23 subunit of the replisome and has a comparable size as other archaeal MCM proteins (8,18). Similar to Tko MCM1 and MCM2, 9°N MCM1 and 9°N MCM2 are also found in mobile elements and contain unique N-terminal extensions that MCM3 lacks (Supplemental Figure S1). Tko MCM1 has minimal DNA unwinding activity (8). Therefore, this study focuses on characterization of the replicative MCM3 and the additional MCM2 from 9°N and the MCM from Mth. These findings contribute to a more comprehensive understanding of the role MCM helicases play in hyperthermophilic archaea and help establish evolutionary links to eukaryotic and bacterial replication systems.

MATERIALS AND METHODS

Materials

Oligonucleotides used in this study were purchased from Integrated DNA Technologies (IDT, Coralville, IA). DNA sequences were as follows: (oligonucleotide 1) leading strand template 5′-PO_4- GGG CGG CGA CCT GGA CAG CAA GTT GGA CAA TCT CGT TCT ATC ACT AAT TCA CTA ATG CAG GGA GGA TTT CAG ATA TGG CA-3′; (oligonucleotide 2) leading strand primer 5′-TGC CAT ATC TGA AAT CCT CCC TGC-3′; (oligonucleotide 3) biotinylated fork arm 5′-biotin-A_{16}GA GTA CTG TAC GAT CTA GCA TCA ATC ACA GGG TCA GGT TCG TTA TTG TCC AAC TTG CTG TCC-3′; (oligonucleotide 4) bead oligonucleotide 5′-PO_4-AGG TCG CCG CCC A_{12}-NH_2-3′. Carboxylic acid functionalized Dynabeads were purchased from Life Technologies (Carlsbad, CA). T7 Express *Escherichia coli* expression cells, lambda (λ) DNA, T7 DNA ligase, T4 DNA ligase, T4 DNA ligase buffer (50 mM Tris–HCl, pH 7.5 at 25°C, 10 mM $MgCl_2$, 1 mM ATP, 10 mM DTT), streptavidin, ThermoPol Buffer [20 mM Tris–HCl, pH 8.8 at 25°C, 10 mM $(NH_4)_2SO_4$, 10 mM KCl, 2 mM $MgSO_4$, 0.1% Triton® X-100], ThermoPol buffer (detergent-free) [20 mM Tris–HCl, 10 mM $(NH_4)_2SO_4$, 10 mM KCl, 2 mM $MgSO_4$, pH 8.8 at 25°C], and ATP were from New England Biolabs, Inc. (NEB, Ipswich, MA, USA). Mth MCM helicase was cloned, over-expressed and purified as described previously (6). 9°N MCM2 and MCM3 helicases were cloned, overexpressed and purified as described below. All chromatography columns for purification were purchased from GE Healthcare (Pittsburgh, PA). Flow cells (Figure 1) were constructed as described in (10) with materials from the following: biotin coated slides, Microsurfaces Inc. (Englewood, NJ); quartz slide, Technical Glass (Painesville, OH); double-sided secure seal tape, Grace Biolabs (Bend, OR, USA); epoxy gel, Devcon (Danvers, MA); and polyethylene tubing, Becton Dickinson (Franklin Lakes, NJ, USA). A cartridge heater, high temperature heat conductivity paste and thermocouples (for

temperature calibration) were purchased from Omega Engineering (Stamford, CT, USA). An aluminum block, used to transfer heat to the flow cell, was constructed by and a generous gift from Joseph Loparo (Harvard Medical School). A variable autotransformer was purchased from Staco, Inc. (Dayton, OH, USA) and a syringe pump, used to introduce flow to the flow cell, was purchased from Kent Scientific (Torrington, CT, USA). Permanent rare earth magnets [Magcraft, Inc. (Vienna, VA)] were used to hold beads above the flow cell surface with a translation stage and homemade mount [ThorLabs, Inc. (Newton, NJ, USA)]. Single-molecule experiments were carried out on a Zeiss Axiovert 200m microscope using Axiovision software.

Cloning, expression and purification of 9°N MCM helicases

The 9°N MCM2 and MCM3 genes were identified in the 9°N draft genome sequence by similarity to other known MCM helicases. 9°N MCM3 contained four inteins (Supplementary Figure S2). The 9°N MCM2 and MCM3 genes (lacking inteins) were codon optimized for expression in *E. coli,* constructed synthetically (Genscript, Piscataway, NJ) and cloned into pAII17 plasmid vector (19) cleaved with NdeI and BamHI to produce plasmids pERN (9°N MCM2) and pEUK (9°N MCM3). NEB T7 Express *E. coli* cells containing plasmids encoding pERN or pEUK were grown at 37°C in one liter of LB media supplemented with 0.1 mg/ml ampicillin. When culture reached an OD_{600} of 0.5, expression of 9°N MCM was induced by addition of 0.4 mM (final concentration) of isopropyl β-D-thiogalactopyranoside (IPTG). Cells were allowed to grow for 3 h in the presence of IPTG, and were collected by centrifugation at 4000 rpm for 15 min. Cell pellets were suspended in buffer A (20 mM Tris–HCl pH 7.5, 0.1% Triton X-100, 5% glycerol) containing 0.25 M NaCl, and lysed by sonication and heating at 80°C for 20 min. Centrifugation was used to remove cell debris. The supernatant was passed through a DEAE column and flow through was collected and diluted with buffer A to 50 mM NaCl. Diluted flow through was loaded onto a Heparin HyperD column, pre-equilibrated with buffer A containing 50 mM NaCl, and eluted with a buffer A gradient from 50 mM to 1 M NaCl. Peak fractions were identified by SDS-PAGE analysis, pooled and diluted in buffer A to 50 mM NaCl. Diluted peak fractions were loaded onto a Heparin TSK column, pre-equilibrated with buffer A containing 50 mM NaCl, and eluted with a buffer A gradient from 50 mM to 1 M NaCl. Peak fractions were identified by SDS-PAGE analysis, pooled and separated by XK50 size exclusion chromatography. Peak fractions were pooled and dialyzed to 10 mM Tris–HCl pH 7.5, 100 mM KCl, 0.1 mM EDTA, 0.1% Triton X-100 and 50% glycerol.

Assembly of single-molecule DNA constructs

DNA constructs were created using 48.5 kb λ-DNA annealed and ligated to oligonucleotides 1–3 as listed above (10) (Figure 1B). Briefly, oligonucleotides 1, 2 and 3 were annealed to λ-DNA in 1× T4 DNA ligase buffer in a 10:200:10:1 molar ratio, ensuring a molar excess of fork oligonucleotides over λ DNA and that all forks were primed. Annealing was performed by incubating substrates
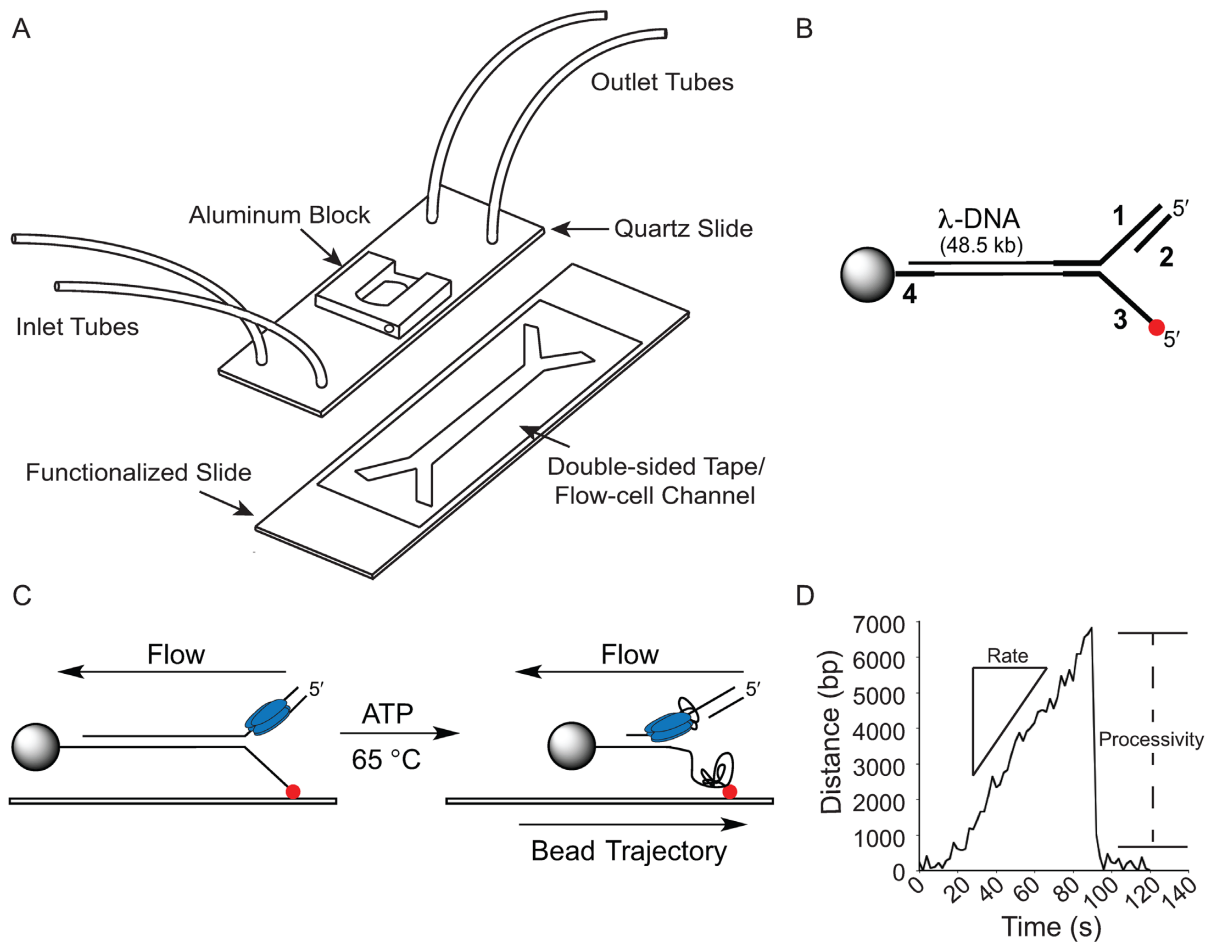
Figure 1. Construction of a thermostable single-molecule flow cell and DNA constructs used for thermostable DNA helicase unwinding experiments. (**A**) A simple flow-cell was constructed from a biotin-streptavidin functionalized slide and a smaller quartz slide, held together by double-sided tape, with a double-Y shape cutout. The quartz slide contains 4 holes holding 25 cm polystyrene tubing, which act as inlet and outlet tubes for delivery and removal of experimental reagents. An aluminum block was placed on top of the quartz slide to act as a housing device for a cartridge heater, which allowed for heating of the flow-cell channel. (**B**) A thermostable DNA-bead construct, which mimics an *in vivo* replication fork, was assembled using λ-DNA, four synthetic oligonucleotides, labeled 1–4, and a functionalized polystyrene bead. (**C**) High-temperature single-molecule reactions were carried out within the flow-cell chamber, where Mth MCM, 9°N MCM2 or 9°N MCM3 (schematically colored in blue) was loaded onto the DNA construct, followed by delivery of ATP to initiate DNA unwinding, at 65°C. Conversion of double-stranded DNA to two single-strands by helicase unwinding leads to movement of the polystyrene bead against laminar flow. (**D**) The trajectory of the polystyrene bead against laminar flow versus time is plotted. The rate of DNA unwinding is extracted from the slope of the unwinding trajectory, and processivity is obtained from the change in bp from start to finish of the DNA unwinding event.

at 65°C for 5 min and slowly cooling to room temperature, and the construct was ligated by incubating with 800 units of T4 DNA ligase for 2 h at room temperature. Carboxylic acid-functionalized magnetic Dynabeads were coupled to oligonucleotide 4 following manufacturer's protocol and stored at 4°C in 1× PBS (137 mM NaCl, 2.7 mM KCl, 10 mM Na_2HPO_4, 2 mM KH_2PO_4), pH 7.4 with 0.1% bovine serum albumin (BSA).

Construction of flow cell chamber

A previously designed flow cell was constructed to carry out single-molecule experiments at 37°C (10) and we modified its design to withstand high temperatures for assays 65°C (Figure 1A). Quartz flow cell tops were prepared by drilling four holes into a 1-mm thick, 2-cm × 5-cm quartz slide. A 3 mm double-Y shaped channel, was cut from

double-sided Secure Seal tape and affixed to the quartz slide. Blocking buffer (20 mM Tris–HCl, pH 7.5, 2 mM EDTA, 50 mM NaCl, 0.2 mg/ml BSA, 0.005% (v/v) Tween-20) was prepared and degassed. For each experiment, a biotin-functionalized slide was incubated with streptavidin (0.2 mg/ml final concentration in blocking buffer) for 30 min at room temperature. The slide was briefly washed with H_2O and dried with compressed air. The tape/quartz slide was then affixed to the functionalized slide. Polyethylene tubing was cut, placed into each of the four quartz slide holes, and secured with epoxy. The bottom of the aluminum heat block was coated with a thin layer of high temperature thermal conductivity paste, and the block was placed on top of the quartz slide and affixed with epoxy. Blocking buffer was pulled through the flow cell and incubated at room temperature for 20 min.

After incubation to block flow cell surfaces, the chamber was placed on an inverted microscope. A cartridge heater was inserted into the drilled hole in the aluminum block and attached to a power source. Temperature calibration was performed by attaching two independent thermocouples to the flow cell, one on the outside notched edge of the aluminum block and another directly in the flow channel to measure buffer temperature in the observation area, accessed by a hole drilled into a quartz calibration slide. Temperature at both positions was measured and voltage on the variable autotransformer was increased until the desired temperature was reached inside the flow cell. Voltage and temperature at both positions were recorded for use in future experiments (Supplementary Figure S3). The variable autotransformer was calibrated to heat the flow cell to a 65°C reaction temperature, and the flow cell remained intact at this high temperature for over 24 h.

MCM DNA unwinding assay and data analysis

The helicase DNA unwinding experiment was adapted from the 'Replication loops with tethered bead motion' protocol in reference (10). The flow cell was connected to an air spring to stabilize flow in line with the syringe pump and placed on the microscope stage as previously described. Biotin-fork λ DNA was flowed through the flow cell in blocking buffer, and incubated in the chamber with no flow for 10 min to maximize DNA capture on the streptavidin coated slide. Next, oligonucleotide 4-beads were ligated to the tethered λ DNA on the flow cells as follows. A diluted oligonucleotide 4-bead aliquot was prepared by adding 10 μl of stock oligonucleotide 4-beads to 288.5 μl of 1× T4 DNA ligase buffer; the oligonucleotide 4-bead aliquot was then vortexed for 30 seconds, and sonicated for 30 s. Following sonication, 1.5 μl of T7 DNA ligase was added and mixed gently, then the bead solution flowed into chamber in cycles of 2 min flow at 32.5 μl/min and no flow for 1 min, repeated 5–8 times to maximize bead annealing and ligation to the tethered forked λ DNA. Following bead attachment, the flow cell was thoroughly washed with blocking buffer with frequent tapping of the microscope stage to dislodge and remove any non-ligated oligonucleotide-beads. Aliquots of 1× ThermoPol buffer (Detergent Free) with and without 1 mM ATP were degassed, and 40 nM of MCM (as monomer) was added to 500 μl of ATP-free buffer ThermoPol buffer was flowed into the chamber and temperature raised to 65°C MCM was then flowed through the heated flow cell at 32.5 μl/min for 3 min followed by 12.5 μl/min for 5 min to allow binding of the helicase to the forked DNA substrates. The flow cell was washed with 1× ThermoPol buffer for 3 min at 12.5 μl/min. Prior to reaction initiation, a magnet was positioned over the flow cell to prevent bead-surface interactions for tethered beads. Initiation of helicase DNA unwinding was achieved by flowing ATP at 12.5 μl/min, corresponding to 3 pN force applied to the DNA constructs. Dark field illumination was used to increase the contrast between the magnetic beads and the background. A time-lapse movie using the Axiovert Axiovision software and a CCD camera monitored the position of the tethered beads at 0.5 s intervals for 2500 frames.

Trajectories of the beads were obtained by analysis of the movies using DiaTrack tracking software and filtered to remove short, aberrant, and untethered trajectories. Trajectories were then visualized and analyzed manually using Origin graphing software. The trajectories, which are imported as the position of pixels created by the polystyrene bead under dark field illumination, are converted into base pairs by using the pixel size of the camera and the measured length of the tethered DNA particles under the described conditions (10). A control single-molecule experiment with φ29 DNA polymerase confirmed consistency between the single-molecule assay system and previously published biochemical studies (11,20–22) (Supplementary Figure S4).

Helicase events were defined by bead movement against flow. Experimental noise was minimized by subtracting a background trajectory (a tethered bead showing no helicase activity) from all analyzed trajectories. Processivity was determined by the total bead distance moved against flow, and rate was determined by a linear fit of bead movement versus time. Only events greater than two times the bead Brownian noise level at 65°C were confidently identified, limiting our observations to unwinding events of 800 bp or greater. Fifty-five unwinding events, obtained from three separate single-molecule experiments for each MCM helicase, were used to obtain reported rates (bp s^{-1}) and processivities (bp). Reported helicase processivities were obtained by binning processivities using Origin and fitting to an exponential decay equation ($y = y_\mathrm{o} + e^{-tx}$), where exponential decay constant 't' represents processivity. The first bin (0–2000) was excluded from exponential decay fitting due to the inability to confidently detect events with short (≤800 bp) processivities (23).

RESULTS

Design of a high temperature single-molecule DNA helicase assay

We designed a single molecule assay to monitor long DNA unwinding events by DNA helicases at a high temperature (65°C) to closely mimic 9°N and Mth physiological growth temperature. In the single molecule flow cell, a constant laminar flow applies a force of 3 pN to the attached DNA constructs. A low stretching force of 3 pN allows for sufficient contrast between the near-crystallographic dsDNA and entropically collapsed ssDNA (9) but below forces seen to affect helicase unwinding when applied directly to unwinding forks (24,25). Specifically, under low force, double-stranded DNA (dsDNA) reaches near its crystallographic length, while single-stranded DNA (ssDNA) collapses upon itself (9,26,27). This length difference has been exploited to observe the activities of DNA enzymes, and it is used here to measure the processive activity of thermostable helicases. The helicase converts duplex DNA to two single strands and this transition to ssDNA causes a polystyrene bead (attached to one strand of the construct) to move against flow (Figure 1C and Supplementary Movie). Therefore, the rate and distance of bead movement corresponds to DNA helicase unwinding activity. Once the helicase dissociates from the DNA construct, the strands rapidly reanneal to form a dsDNA molecule. The position of each bead is converted to a trajectory as the change in length of the DNA over time,

giving rise to a distinct DNA unwinding profile, previously referred to as a saw-tooth pattern (24) (Figure 1D).

From one single-molecule experiment, 25–50 individual helicase DNA unwinding events can be observed. From each DNA unwinding event, two parameters are obtained: the rate of DNA unwinding (in bp s^{-1}), and the helicase processivity, or total number of bases unwound by the helicase (Figure 1D). The rate at which the helicase has unwound the DNA is obtained from the slope ($\Delta y/\Delta x$) of the DNA shortening trajectory, while the processivity is obtained by the change in bp from the start to end of DNA unwinding (Figure 1D).

DNA unwinding activities of Mth MCM, 9°N MCM2 and MCM3 helicases

The Mth genome encodes a single MCM homolog responsible for unwinding the chromosomal DNA during replication. Mth MCM unwinds DNA at rate of 52 ± 8 bp s^{-1} with a processivity of 3900 ± 480 bp (Figure 2, Table 1). 9°N encodes one replicative MCM3 and two additional MCM homologs (MCM1, MCM2). The replicative 9°N MCM3 unwinds DNA at a faster rate, 162 ± 10 bp s^{-1}, compared to the 9°N MCM2, 42 ± 5 bp s^{-1} (Figure 2, Table 1). Despite differences in unwinding rates, 9°N MCM2 and MCM3 share similar processivities of 4700 ± 350 bp and 4500 ± 220 bp, respectively (Table 1). Importantly, the processivity and rate of unwinding do not correlate with one another for any of the three helicases. For example, longer processivity is not linked to a faster unwinding rate, and vice versa, indicating independent activities (Supplementary Figure S5). Interestingly, in ~5–10% of unwinding events for all helicases studied, two consecutive saw-tooth patterned trajectories are observed suggesting two successive unwinding events by a single MCM (a representative trace is shown in Figure 3A). Helicase unwinding rate, processivity and observed fraction of slippage events are independent of 9°N MCM3 concentration suggesting that single or multiple trajectories were the action of a single helicase (Supplementary Figure S6).

The helicase activities displayed significant variation and reflects the underlying stochastic nature of the unwinding reaction. For example, while the average rate of Mth DNA unwinding was 52 ± 8 bp s^{-1}, a small number of faster events were also observed (up to 123 bp s^{-1}). Similarly, even though the majority of unwinding events had an unwinding processivity of ~4 kb, we also observed a fraction of longer DNA unwinding events over 10 kb (Figure 2E–H). The heterogeneity in unwinding and processivity within the population of helicases highlights the utility of the single-molecule assay to provide unique insights into reaction intermediates and mechanism.

DISCUSSION

Comparison of DNA unwinding rates and processivities of archaeal and other replicative helicases

The adaptation of the single-molecule bead assay to study high temperature thermostable enzymes provides insight into the kinetics of processive DNA helicases. Single-molecule assays have been used to observe the unwinding kinetics of a variety of DNA helicases including those from bacteriophages T4 and T7 and *E. coli* (24,25,28,29). The rate of DNA unwinding for helicases ranges from 30 bp s^{-1} for T4 gp41, 50 bp s^{-1} for *E. coli* DnaB to as fast as 250 bp s^{-1} for T7 gp4 (24,25,28,29). The Mth MCM and 9°N MCM2 unwinding rates were similar (52 ± 8 bp s^{-1} and 42 ± 5 bp s^{-1}, respectively) to T4 gp41 and *E. coli* DnaB while 9°N MCM3 was similar to T7 gp4, suggesting a large diversity of helicase unwinding rates across organisms. This diversity is likely the result of varied helicase structures, other proteins and factors that regulate helicase activity *in vivo* and growth environments. Furthermore, the notable difference observed in unwinding rate between 9°N MCM2 and MCM3 is likely due to the presence of the N-terminal extension on MCM2 (Supplementary Figure S1), which may inhibit or slow helicase progression. Indeed, truncation of the N-terminal extension of Tko MCM2 lead to a significant increase in helicase DNA unwinding activity (8), providing further support that the N-terminal extension regulates MCM2 DNA unwinding rates.

According to current models, replication in Mth and Tko initiate at a single origin of replication and two replisome complexes synthesize the genome bidirectionally to produce two copies of the chromosome. To ensure each new cell has a complete genome, replication must occur before cell division. Based on a 300 minute doubling time at 65°C, the overall Mth genome replication rate should be at least 49 bp s^{-1} per replisome (13,14). Interestingly, the Mth MCM unwinding rate (52 ± 8 bp s^{-1}) parallels the estimated Mth genome replication rate. Similarly, the 9°N MCM3 unwinding rate (162 ± 10 bp s^{-1}) is comparable to the estimated genome replication rate (180 nt s^{-1} per replisome) of closely related *Thermococcus* strain (Tko) growing at 85°C (30,31). These data support the prediction that the 9°N MCM2 homolog is unlikely to be the main replicative MCM since it is at least four times slower (42 ± 5 bp s^{-1}) than the estimated genome replication rate. Together these data suggest that overall *in vivo* genome replication speed may be determined in part by the rate of MCM replication fork unwinding. However, additional studies are required to address the influence of other replication and chromatin proteins that may influence replication rates.

DNA helicases from bacteriophage T4 and T7 and *E. coli* DnaB are loaded on the lagging strand and have relatively low processivities, ranging from 100 to 800 bp (24,25,28,29) while Mth MCM, 9°N MCM2 and MCM3 are much more processive ($4,700 \pm 350$, $4,500 \pm 220$ and $3,900 \pm 480$, respectively). These data suggest MCM helicases loaded on the leading strand may have higher inherent processivity than helicases loaded onto the lagging strand. However, other replication proteins likely regulate helicase processivity. For example, in isolation, T7 gp4 helicase processivity is 500 bp; the T7 replisome complex processivity increases to 17 kb in a single binding event (24,32). Similarly, longer DNA unwinding is observed by the entire *E. coli* replisome complex compared to DnaB alone (27,33). Therefore other archaeal replisome components such as GAN, GINS, DNA polymerase or other proteins may further regulate MCM processivity (34).
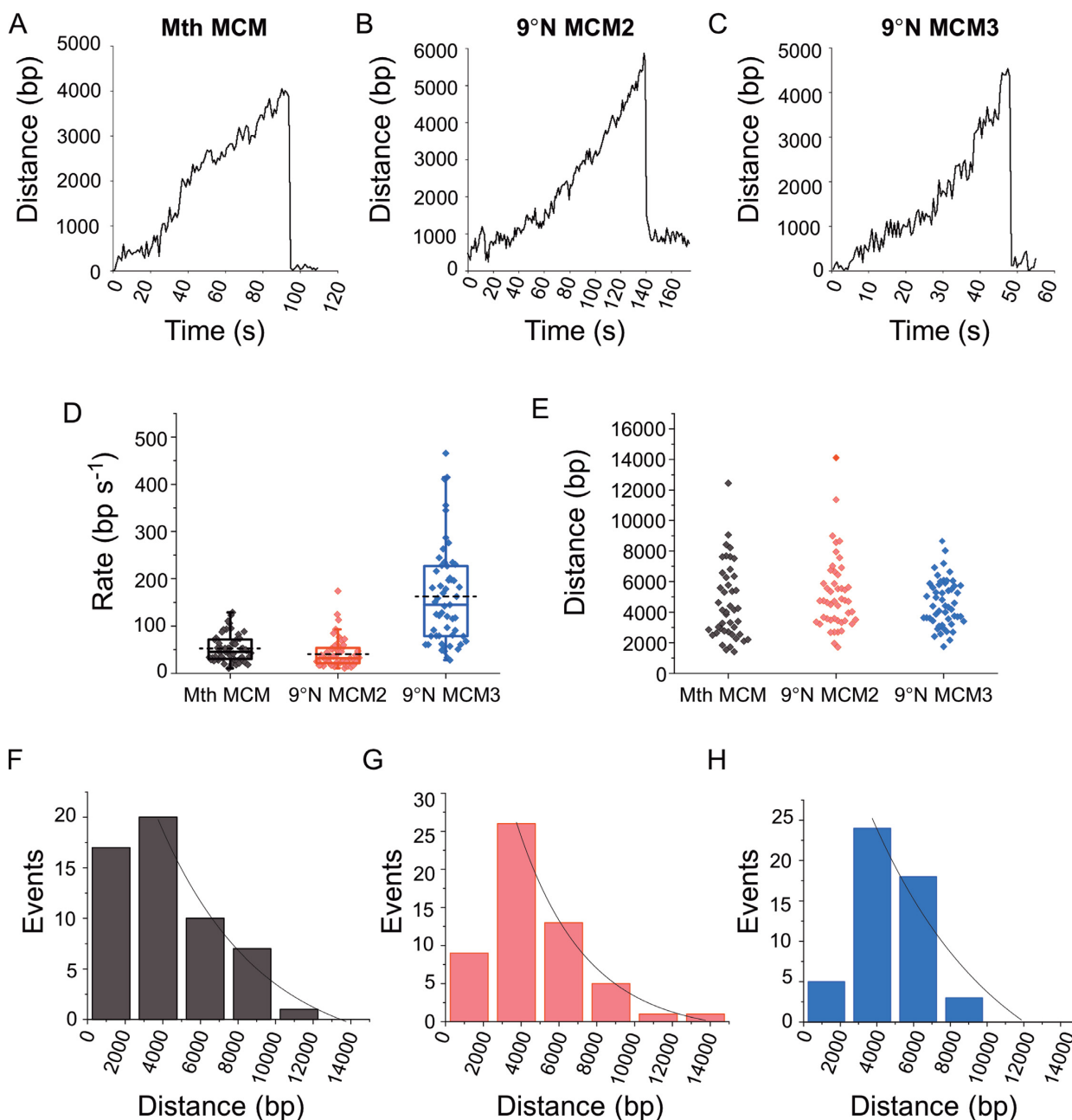
Figure 2. DNA unwinding trajectories and kinetic parameters from single molecule helicase unwinding events. A representative single molecule DNA unwinding trajectory for (**A**) Mth MCM, (**B**) 9°N MCM2 and (**C**) 9°N MCM3 is shown. (**D**) Mth MCM (black), 9°N MCM2 (red) and 9°N MCM3 (blue) single-molecule unwinding rates are plotted. Each point is a rate from a single unwinding event. The vertical box represents the 25–75% range and dotted line is the mean unwinding rate. The vertical whiskers denote the 5–95% range of the data. (**E**) Mth MCM (black), 9°N MCM2 (red) and 9°N MCM3 (blue) single-molecule unwinding processivities are plotted. Each point is the processivity from a single unwinding event. Processivity data from single data points were binned and fit to a single-exponential decay. (**F**) Mth MCM (black) processivity. (**G**) 9°N MCM2 (red) processivity. (**H**) 9°N MCM3 (blue) processivity.

Table 1. Kinetic parameters of DNA unwinding by Mth MCM, 9°N MCM2 and 9°N MCM3[a]

Enzyme	Processivity (bp)	Unwinding rate (bp s^{-1})
Mth MCM	3900 ± 480	52 ± 8
9°N MCM2	4700 ± 350	42 ± 5
9°N MCM3	4500 ± 220	162 ± 10

[a]Kinetic parameters are obtained from the average of 55 DNA unwinding events ± standard error.
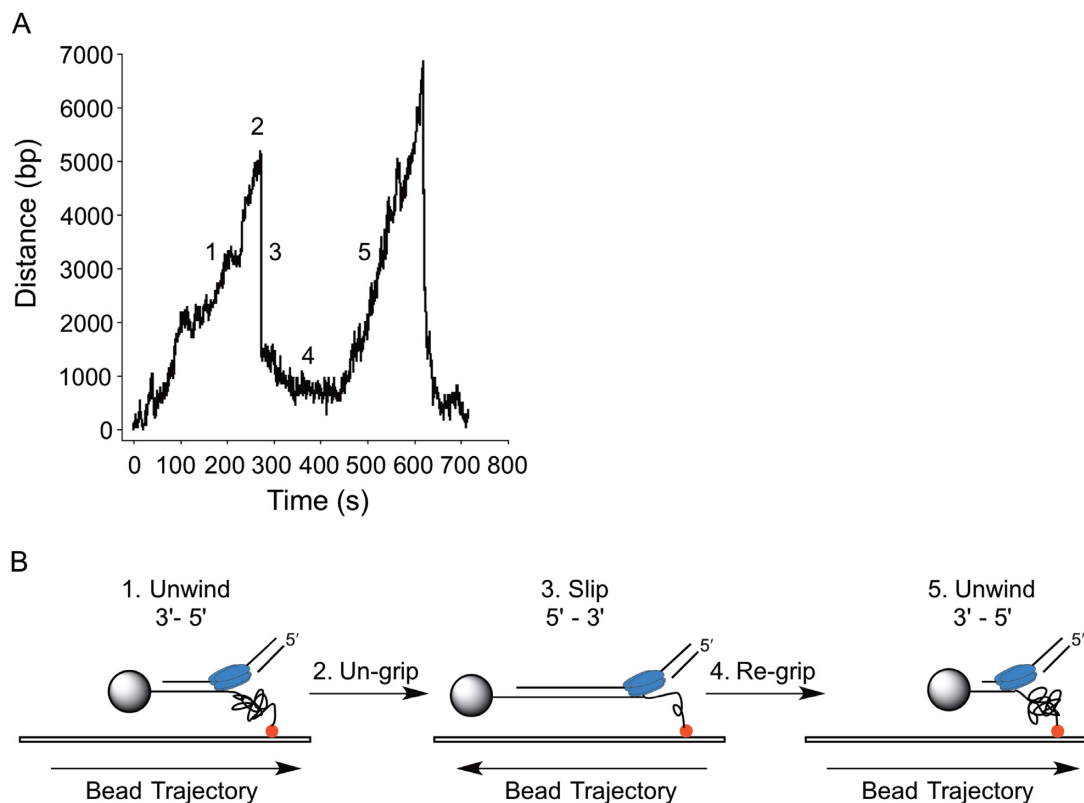
Figure 3. DNA helicase slippage trajectory and reaction scheme. (**A**) In 5–10% of DNA unwinding events, DNA slippage by the helicase is observed, as exhibited by two successive DNA unwinding trajectories by 9°N MCM2. A representative single molecule DNA unwinding trajectory is shown. (**B**) We propose the helicase (1) unwinds the DNA, (2) loses its grip on the construct, (3) slides back in a 5′-3′ direction, (4) regains its grip (5) and unwind the DNA a second time, followed by dissociation of the helicase from the DNA.

Helicase dissociation and slippage events

The trajectories obtained from DNA unwinding events create a distinct saw-tooth pattern that are characteristic of DNA helicases analyzed by a variety of single-molecule assays (Figure 3A) (24,25,28,29,35). While bead movement against flow is attributed to DNA unwinding by the helicase, it is likely that the rapid repositioning phase of the bead to its original location is due to the dissociation of the helicase from the DNA. This dissociation would allow for rapid reannealing of the two single-strands to double stranded DNA. We propose that in the 5–10% of events in which two successive DNA unwinding events occur (a representative trace is shown in Figure 3A) that after the first DNA unwinding event, the MCM loses its grip on the DNA but does not dissociate, slips back in a 5′-3′ direction, regains its grip on the DNA and catalyzes another unwinding event (Figure 3B) (24). *In vivo*, a DNA helicase is linked to DNA polymerase synthesis, and therefore the translocation observed here might be the result of a DNA helicase in isolation without a DNA polymerase to prevent slipping back. Factors that influence MCM unwinding and slipping and possible biological relevance in replication and replication restart will require further study.

Although it possible that two different helicase molecules successively binding to the same DNA construct and produce two successive trajectories, it is highly unlikely due to several factors. First, the frequency of tethered beads dis-

playing helicase activity is relatively low, and the likelihood of multiple independent associations is accordingly much lower. Also the free concentration of MCM helicase within the flow cell is very low due to preassembly without ATP and removal of free helicase by extensive washing. Additionally the size of the replication fork structure is only 49 bases, sufficient to accommodate only a single MCM per substrate during initial binding.

Future studies should shed light on the consequences of DNA sequence context, the presence of DNA lesions or DNA binding proteins on thermostable DNA helicase processivity. Within the context of the cell, the helicase functions in a concerted fashion with many accessory proteins, including Cdc45, DNA primase, DNA polymerases and the GINS complex, that likely influence helicase activity. The single-molecule analysis reported here may accelerate understanding DNA unwinding mechanisms of thermophilic organisms.

SUPPLEMENTARY DATA

Supplementary Data are available at NAR Online.

REFERENCES

1. Slaymaker,I.M. and Chen,X.S. (2012) MCM structure and mechanics: what we have learned from archaeal MCM. *Subcell. Biochem.*, **62**, 89–111.
2. Costa,A. and Onesti,S. (2009) Structural biology of MCM helicases. *Crit. Rev. Biochem. Mol. Biol.*, **44**, 326–342.
3. Brewster,A.S. and Chen,X.S. (2010) Insights into the MCM functional mechanism: lessons learned from the archaeal MCM complex. *Crit. Rev. Biochem. Mol. Biol.*, **45**, 243–256.
4. Sakakibara,N., Kelman,L.M. and Kelman,Z. (2009) Unwinding the structure and function of the archaeal MCM helicase. *Mol. Microbiol.*, **72**, 286–296.
5. Chong,J.P., Hayashi,M.K., Simon,M.N., Xu,R.M. and Stillman,B. (2000) A double-hexamer archaeal minichromosome maintenance protein is an ATP-dependent DNA helicase. *Proc. Natl. Acad. Sci. U.S.A.*, **97**, 1530–1535.
6. Kelman,Z., Lee,J.K. and Hurwitz,J. (1999) The single minichromosome maintenance protein of *Methanobacterium thermoautotrophicum* ΔH contains DNA helicase activity. *Proc. Natl. Acad. Sci. U.S.A.*, **96**, 14783–14788.
7. Krupovic,M., Gribaldo,S., Bamford,D.H. and Forterre,P. (2010) The evolutionary history of archaeal MCM helicases: a case study of vertical evolution combined with hitchhiking of mobile genetic elements. *Mol. Biol. Evol.*, **27**, 2716–2732.
8. Pan,M., Santangelo,T.J., Li,Z., Reeve,J.N. and Kelman,Z. (2011) *Thermococcus kodakarensis* encodes three MCM homologs but only one is essential. *Nucleic Acids Res.*, **39**, 9671–9680.
9. van Oijen,A.M. (2007) Honey, I shrunk the DNA: DNA length as a probe for nucleic-acid enzyme activity. *Biopolymers*, **85**, 144–153.
10. Tanner,N.A. and van Oijen,A.M. (2010) Visualizing DNA replication at the single-molecule level. *Methods Enzymol.*, **475**, 259–278.
11. Kim,S., Blainey,P.C., Schroeder,C.M. and Xie,X.S. (2007) Multiplexed single-molecule assay for enzymatic activity on flow-stretched DNA. *Nat. Methods*, **4**, 397–399.
12. Yodh,J.G., Schlierf,M. and Ha,T. (2010) Insight into helicase mechanism and function revealed through single-molecule approaches. *Q. Rev. Biophys.*, **43**, 185–217.
13. Zeikus,J.G. and Wolfe,R.S. (1972) *Methanobacterium thermoautotrophicus* sp. n., an anaerobic, autotrophic, extreme thermophile. *J. Bacteriol.*, **109**, 707–715.
14. Smith,D.R., Doucette-Stamm,L.A., Deloughery,C., Lee,H., Dubois,J., Aldredge,T., Bashirzadeh,R., Blakely,D., Cook,R., Gilbert,K. *et al.* (1997) Complete genome sequence of *Methanobacterium thermoautotrophicum* ΔH: functional analysis and comparative genomics. *J. Bacteriol.*, **179**, 7135–7155.
15. Southworth,M.W., Kong,H., Kucera,R.B., Ware,J., Jannasch,H.W. and Perler,F.B. (1996) Cloning of thermostable DNA polymerases from hyperthermophilic marine Archaea with emphasis on *Thermococcus* sp. 9°N-7 and mutations affecting 3′-5′ exonuclease activity. *Proc. Natl. Acad. Sci. U.S.A.*, **93**, 5281–5285.
16. Schermerhorn,K.M. and Gardner,A.F. (2015) Pre-steady-state kinetic analysis of a Family D DNA polymerase from *Thermococcus* sp. 9°N reveals mechanisms for archaeal genomic replication and maintenance. *J. Biol. Chem.*, **290**, 21800–21810.
17. Greenough,L., Kelman,Z. and Gardner,A.F. (2015) The roles of family B and D DNA polymerases in *Thermococcus* species 9°N Okazaki fragment maturation. *J. Biol. Chem.*, **290**, 12514–12522.
18. Ishino,S., Fujino,S., Tomita,H., Ogino,H., Takao,K., Daiyasu,H., Kanai,T., Atomi,H. and Ishino,Y. (2011) Biochemical and genetical analyses of the three MCM genes from the hyperthermophilic archaeon, *Thermococcus kodakarensis*, *Genes Cells*, **16**, 1176–1189.
19. Kong,H., Kucera,R.B. and Jack,W.E. (1993) Characterization of a DNA polymerase from the hyperthermophile archaea *Thermococcus litoralis*. Vent DNA polymerase, steady state kinetics, thermal stability, processivity, strand displacement, and exonuclease activities. *J. Biol. Chem.*, **268**, 1965–1975.
20. Blanco,L. and Salas,M. (1985) Replication of phage φ29 DNA with purified terminal protein and DNA polymerase: synthesis of full-length φ29 DNA. *Proc. Natl. Acad. Sci. U.S.A.*, **82**, 6404–6408.
21. Blanco,L., Bernad,A., Lazaro,J.M., Martin,G., Garmendia,C. and Salas,M. (1989) Highly efficient DNA synthesis by the phage φ29 DNA polymerase. Symmetrical mode of DNA replication. *J. Biol. Chem.*, **264**, 8935–8940.
22. Blasco,M.A., Lázaro,J.M., Bernad,A., Blanco,L. and Salas,M. (1992) φ29 DNA polymerase active site. Mutants in conserved residues Tyr254 and Tyr390 are affected in dNTP binding. *J. Biol. Chem.*, **267**, 19427–19434.
23. Schnitzer,M.J. and Block,S.M. (1995) Statistical kinetics of processive enzymes. *Cold Spring Harb. Symp. Quant. Biol.*, **60**, 793–802.
24. Sun,B., Johnson,D.S., Patel,G., Smith,B.Y., Pandey,M., Patel,S.S. and Wang,M.D. (2011) ATP-induced helicase slippage reveals highly coordinated subunits. *Nature*, **478**, 132–135.
25. Ribeck,N., Kaplan,D.L., Bruck,I. and Saleh,O.A. (2010) DnaB helicase activity is modulated by DNA geometry and force. *Biophys. J.*, **99**, 2170–2179.
26. Hamdan,S.M., Johnson,D.E., Tanner,N.A., Lee,J.-B., Qimron,U., Tabor,S., van Oijen,A.M. and Richardson,C.C. (2007) Dynamic DNA helicase-DNA polymerase interactions assure processive replication fork movement. *Mol. Cell*, **27**, 539–549.
27. Tanner,N.A., Hamdan,S.M., Jergic,S., Loscha,K.V., Schaeffer,P.M., Dixon,N.E. and van Oijen,A.M. (2008) Single-molecule studies of fork dynamics in *Escherichia coli* DNA replication. *Nat. Struct. Mol. Biol.*, **15**, 170–176.
28. Lionnet,T., Spiering,M.M., Benkovic,S.J., Bensimon,D. and Croquette,V. (2007) Real-time observation of bacteriophage T4 gp41 helicase reveals an unwinding mechanism. *Proc. Natl. Acad. Sci. U.S.A.*, **104**, 19790–19795.
29. Sun,B., Wei,K.J., Zhang,B., Zhang,X.H., Dou,S.X., Li,M. and Xi,X.G. (2008) Impediment of *E. coli* UvrD by DNA-destabilizing force reveals a strained-inchworm mechanism of DNA unwinding. *EMBO J.*, **27**, 3279–3287.
30. Matsuno,Y., Sugai,A., Higashibata,H., Fukuda,W., Ueda,K., Uda,I., Sato,I., Itoh,T., Imanaka,T. and Fujiwara,S. (2009) Effect of growth temperature and growth phase on the lipid composition of the archaeal membrane from *Thermococcus kodakaraensis*. *Biosci. Biotechnol. Biochem.*, **73**, 104–108.
31. Fukui,T., Atomi,H., Kanai,T., Matsumi,R., Fujiwara,S. and Imanaka,T. (2005) Complete genome sequence of the hyperthermophilic archaeon *Thermococcus kodakaraensis* KOD1 and comparison with *Pyrococcus* genomes. *Genome Res.*, **15**, 352–363.
32. Lee,J.B., Hite,R.K., Hamdan,S.M., Xie,X.S., Richardson,C.C. and van Oijen,A.M. (2006) DNA primase acts as a molecular brake in DNA replication. *Nature*, **439**, 621–624.
33. Yao,N.Y., Georgescu,R.E., Finkelstein,J. and O'Donnell,M.E. (2009) Single-molecule analysis reveals that the lagging strand increases replisome processivity but slows replication fork progression. *Proc. Natl. Acad. Sci. U.S.A.*, **106**, 13236–13241.
34. Li,Z., Kelman,L.M. and Kelman,Z. (2013) *Thermococcus kodakarensis* DNA replication. *Biochem. Soc. Trans.*, **41**, 332–338.
35. Byrd,A.K., Matlock,D.L., Bagchi,D., Aarattuthodiyil,S., Harrison,D., Croquette,V. and Raney,K.D. (2012) Dda helicase tightly couples translocation on single-stranded DNA to unwinding of duplex DNA: Dda is an optimally active helicase. *J. Mol. Biol.*, **420**, 141–154.